Published in final edited form as:
Acta Biomater. 2014 July ; 10(7): 3108–3116. doi:10.1016/j.actbio.2014.03.011.

Alternative strategies to manipulate fibrocyte involvement in the fibrotic tissue response: pharmacokinetic inhibition and the feasibility of directed-adipogenic differentiation

David W Baker[1], **Yi-Ting Tsai**[1], **Hong Weng**[1], and **Liping Tang**[1,2]

[1]Bioengineering Department, University of Texas at Arlington, Arlington, TX 76019-0138

[2]Department of Biomedical Science and Environmental Biology, Kaohsiung Medical University, Kaohsiung 807, Taiwan

Abstract

Fibrocytes have previously been identified as important mediators in several inflammatory and fibrotic diseases. However, there is no effective treatment thus far to reduce fibrotic tissue responses without affecting wound healing reactions. Here we investigate two strategies to alleviate fibrocyte interactions at the biomaterial interface reducing collagen production and scar tissue formation. First, in an indirect approach, TGF-β inhibitor-SB431542 and IL-1β/TNF-α inhibitor SB203580 were locally released from scaffold implants to block their respective signaling pathways. We show that inhibition of IL-1β/TNF-α has no influence on overall fibrotic tissue reactions to the implants. However, the reduction of localized TGF-β significantly decreases the fibrocyte accumulation and myofibroblast activation while reducing the fibrotic tissue formation. Since fibrocytes can be differentiated into non-fibrotic cell types, such as adipocytes, we further sought a more direct approach to reduce fibrocyte responses by directing fibrocyte differentiation into adipocytes. Interestingly, by initiating fibrocyte-to-adipocyte differentiation through sustained differentiation cocktail release, we find that adipogentic differentiation forces incoming fibrocytes away from the traditional myofibroblast lineage leading to a substantial reduction in the collagen formation and fibrotic response. Our results support a novel and effective strategy to improve implant safety by reducing implant-associated fibrotic tissue reactions via directing non-fibrotic differentiation of fibrocytes.

Keywords

Fibrocyte; Fibrosis; Differentiation; Adipocyte; Foreign body response

Correspondence to Liping Tang, Ph.D., Department of Bioengineering, University of Texas at Arlington, Box 19138, Arlington, TX 76019-0138, phone: 817-272-6075 fax: 817-272-2251 ltang@uta.edu.

1 Introduction

The localized fibrotic response to biomaterials continues to be an ever daunting challenge in the design of artificial implants. It is recognized that the degree of inflammation and the persistence of inflammatory cells and products at the interface may drive the resulting long term fibrotic response to the implant. Unfortunately the interactions between inflammation and fibrotic responses are poorly understood. It is well established that the interactions of immune cells (neutrophils, macrophages, and mast cells) with the biomaterial, prompt the release of a variety of pro-inflammatory and pro-fibrotic cytokines [1–5]. Some of these mediators, including interleukin-1β (IL-1β), tumor necrosis factor-α (TNF-α), platelet activating factor, and platelet-derived growth factor (PDGF) have been shown to prompt the recruitment and activation of fibroblasts which may lead to localized fibrotic tissue formation and collagen production [6–9]. Fibroblasts, however often have organ-specific functions in promoting tissue homeostasis such as extracellular matrix and cytokine production [10]. In addition, fibroblasts are often quiescent in tissue and must activate to myofibroblasts before participating in wound healing or tissue remodeling [11]. Recent evidence suggests that circulating fibroblast-like cells termed fibrocytes may be responsible for the extent of fibrotic reactions, presenting an alternative model of repair. These cells are highly migratory and have been shown to be multi-potent, differentiating to myofibroblasts as well as adipocytes [12–13]. More importantly, these cells have been shown to be responsive to immune/inflammatory cells, migrating with the inflammatory cascade, and reactive to the initiating response of mast cells [14]. In addition, fibrocyte recruitment corresponds directly with the amount of collagen production in wound healing and pulmonary fibrosis [14–15]. By manipulating these versatile fibroblast-like cells, either through upstream immune/inflammatory cell interactions, or through altered differentiation aspects, it may be possible to reduce localized collagen formation and alleviate the fibrotic response.

TGF-β is a well known inflammatory and fibrotic mediator shown to promote pro-fibrotic and wound healing responses [16–18]. In addition, the cytokine has previously been linked to fibrocyte migration and proliferation in a lung fibrosis model [18–20]. Furthermore, TGF-β can also influence myofibroblast differentiation of resident tissue fibroblasts, which may be perpetuated by circulating fibrocytes leading to extensive collagen production [12, 21–22]. To alter fibrocyte mediated responses and their innate differentiation to myofibroblasts, porous tissue scaffolds were made to release TGF-β inhibitor SB431542 using a fabrication technique established previously in our laboratory [23]. SB431542 is a potent ALK-5 inhibitor which has been shown to protect the cardiac conduction system in Chagas' disease, inhibit scar formation after glaucoma surgery, and inhibit extracellular matrix formation of fibronectin and collagen *in vitro* [24–26]. We therefore explore both the acute and long-term response of fibrocytes and their involvement on the degree of biomaterial-mediated fibrotic reactions during localized inhibition of TGF-β. Similarly, SB203580 is a p38 MAPK inhibitor shown to be effective at inhibiting inflammatory agents such as IL-1β and TNF-α [27–28]. SB203580 has been shown to suppress the development of endometriosis, improve renal disease, alleviate arthritis, and reduce bone resorption in rodent models by down-regulating pro-inflammatory cytokines [27, 29–30]. In the inflammatory/ fibrotic cascade

there is a known up-regulation of IL-1β and TNF-α after adhesion of monocytes to material surfaces [5]. IL-1β may further be a potent mitogen for fibrocytes [31], and function to maintain fibrocytes in a pro-inflammatory state driving further recruitment of inflammatory cells [32]. Therefore we also assess the influence of localized SB203580 release from scaffolds.

In an alternative strategy, we investigate the influence of localized fibrocyte-to-adipocyte differentiation on fibrotic tissue reactions surrounding the implant. Fibrocytes have recently been shown to possess differential plasticity with the ability to differentiate not only to myofibroblasts but also adipocytes [12, 33], osteoblasts [34], and chondrocytes [34]. The differentiation of fibrocytes to these various lineages however has so far only been investigated *in vitro*. It is unclear whether fibrocyte differentiation to myofibroblasts is essential to implant-associated fibrotic tissue reactions. To test this hypothesis, fibrocyte myofibroblast differentiation was drastically reduced by inducing adipogenic differentiation with sustained release of a specific mitogenic cocktail. The feasibility of this approach is supported by several lines of evidence. First, human fibroblasts have been characterized to have myofibroblastic or lipofibroblastic phenotypes with Thy−1+ and Thy−1− subsets [35]. Second, it has been shown *in vitro*, that differentiation of fibrocytes to adipocytes is driven by the peroxisome proliferator-activated receptor PPAR-γ and that TGF-β drives fibrocyte-to-myofibroblast differentiation [12]. Interestingly the two pathways were found to have reciprocal inhibition of each other [12, 36]. This paradigm was investigated both in vitro and in vivo.

2 Materials and Methods

2.1 Materials

All chemicals were purchased from Sigma-Aldrich (St Louis, MO) unless otherwise specified. Poly (D,L-lactic-co-glycolic acid) (75:25, 113kDa) was purchased from Medisorb Inc., (Birmingham, AL). The near-infrared fluorophore Xsight 761 was obtained from Carestream Health, (New Haven, CT). Mini-osmotic pumps (Alzet Model 1002) were purchased from Alza Corporation, (Palo Alsot, CA) and the corresponding polyvinyl chloride catheters were also obtained from Alzet (Durect Corporation, Cupertino, CA). For differentiation studies, StemPro Adipogenesis Differentiation media (Kit A10070-01) was purchased from Invitrogen, (Grand Island, NY). Both antagonistic compounds SB431542 and SB203580 were obtained from Selleck Chemicals, (Houston, TX). All primary antibodies were purchased from Santa Cruz Biotech (Santa Cruz, CA) and all secondary antibodies were obtained from ProSci, (Poway, CA).

2.2 Fibrocyte culture and Differentiation

Isolation and culture of fibrocytes was performed by an established procedure in which cells are harvested from the spleens of Balb/c mice [37]. Briefly, the spleen is finely diced and then digested with collagenase (Invitrogen, Grand Island, NY) and hyaluronidase for 30 minutes at 37°C. RPMI media is then used to dilute the sample for cell straining and centrifugation. The sample is then re-suspended in 1ml of red blood cell lysis buffer (155 mM NH_4Cl, 12 mM $NaHCO_3$, 0.1 mM EDTA) for 3 minutes at room temperature. Cell lysis

is neutralized by the addition of phosphate buffer (PBS) before being further cultured. The cells are cultured in DMEM supplemented with M-CSF and IL-13 as previously described for 7 days [37]. Fibrocytes were then positively identified by surface markers CD45 and Collagen 1 (Santa Cruz Biotechnology) through immunohistochemistry. For *in vivo* imaging, some cells were incubated with 5μM of near-infrared fluorophore (Xsight 761) for 3hrs. Following labeling 2×10^6 cells in 200μl PBS were administered by iv injection as described in the previous work [38–39].

For adipogenesis differentiation studies, fibrocytes were subcultured after the initial 7 days in culture and re-plated on glass cover slips in a 24 well plate. Cells were plated at 10,000 cells/well and allowed to adhere overnight. StemPro Adipogenesis Differentiation media was then used, as per the manufacturer's instruction, to stimulate adipogenic differentiation. The media was replaced every 3 days by removing half the old media and supplementing with an equal volume of new media. Differentiation of fibrocytes to adipocytes was carried out for 14 days. Control cells were similarly seeded and supplemented with a half change of media every three days, maintained in the original fibrocyte media containing M-CSF and IL-13. Adipocyte differentiation was confirmed through Oil Red O staining for lipid droplet accumulation. To assess the degree of differentiation some samples were stained with Oil Red O for lipids while other samples were stained with Sirius Red to identify collagen. The two stains were then extracted from the cells and the degree of staining was assessed by colorimetric absorbance micro-assay as previously described [40–41]. Briefly, Oil Red O was extracted by the addition of isopropyl alcohol to the cells. The absorbance of the dye was then read at a wavelength of 510nm on a microplate reader (Infinite® M200; Tecan Group Ltd, Mannedorf, Switzerland). For the Sirius Red assay, the dye was extracted by the addition of a 0.1 N sodium hydroxide solution and read at a wavelength of 550nm.

2.3 Scaffold synthesis and characterization

Protein microbubble scaffolds were used as a model implants capable of releasing anti-inflammatory agents in a controlled fashion. Microbubble scaffold formation was based on our previous method for albumin (BSA) microbubble scaffolds [23]. Briefly, poly (D,L-lactic-co-glycolic acid) (75:25, 113kDa), was dissolved in 1,4-dioxane at a 7.5% w/v ratio. Microbubbles of bovine gelatin were produced by ultra-sonication at 20kHz for 10s of a 10% w/v gelatin solution under nitrogen gas. The resulting gelatin microbubbles were immediately added to the polymeric solution at a 1:1 v/v ratio. The quasi-stable mixture is agitated gently and then quenched in liquid nitrogen to induce phase separation. The scaffolds are then lyophilized (Freezone 12 lyophilizer, Labconco, Kansas City, MO) for 48 hours at 0.03 mbar vacuum. Scaffolds were cut into 5 × 5 × 5 mm cubes and stored at −20°C until implantation. Characterization of gelatin microbubble scaffolds was performed as previously reported in our earlier works [23].

To alter fibrocyte responses two separate inhibitors were incorporated into and released from microbubble scaffolds. Specifically, the TGF-β antagonistic agent SB431542 loaded into scaffolds at a dose of 10 mg/kg body wt/day [24]. Additionally, the IL-1β/TNF-α antagonistic agent SB203580 was loaded into scaffolds at a dose of 15 mg/kg body wt/day [27]. For incorporation into protein microbubble scaffolds the drugs were first solubalized in

dimethylsulfoxide (DMSO) and then blended with the polymer solution just prior to the addition of the protein microbubbles. The drugs were incorporated at 1.4 mg for SB431542 and 2.1 mg for SB203580, per ml polymer solution. The release kinetics of the incorporated drugs were calculated by high performance liquid chromatography (HPLC). HPLC analysis was carried out on a Waters 2695 separations module with a Waters 2996 Photodiode Array Detector (Waters Corp. Milford, MA). The system consisted of a Symmetry C18, 3.5μm 4.6 ×75 mm column with a flow rate of 1ml/min under a gradient flow. The mobile phase consisted of 90% water with 0.1% trifluroacetic acid and 10% acetonitrile.

2.4 Animal models

Balb/c mice (25g body weight) (Harlan, Indianapolis, IN) were selected for equal age and sex prior to implantation. For scaffold implantation, mice were anesthetized and a dorsal midline incision was created as previously described [39]. Briefly, each mouse was implanted with two scaffolds (drug-loaded or drug-free scaffolds), placed laterally on either side of the incision tucked into the subcutaneous space approximately 15mm away from the incision. The incision was then sutured closed. The mice were subsequently returned to housing and monitored daily for irritation around the implant.

In our second model of directed fibrocyte differentiation, mini-osmotic pumps (Alzet Model 1002) were used to achieve sustained delivery of differentiation factors *in vivo*. The pumps are set to deliver a concentrated adipogenic cocktail (StemPro, Invitrogen) at a constant rate of 0.25 ng/h for 14 days. The cocktail consisted of a 40% adipogenic supplement in basal medium prepared from the components in the adipocyte differentiation media from StemPro. The pump was then connected to the microbubble scaffold via a polyvinyl chloride catheter. Both scaffold and pump were then implanted in the subcutaneous cavity of Balb/C mice. The pump was placed into the subcutaneous space away from the incision toward the hind limb. The accompanying scaffold was similarly placed away from the incision toward the center of the back on the same side as the pump. Control scaffolds were placed contralateral to the test scaffold sample. All animals were cared for in compliance with the protocols approved by the Institutional Animal Care and Use Committee at the University of Texas at Arlington.

2.5 Imaging analysis

To quantify the extent of fibrocyte recruitment, whole body animal imaging analyses was carried out using the KODAK in vivo FX Pro system (Kodak, USA). Fluorescence intensity was monitored at excitation wavelength of 760 nm and emission wavelength of 790 nm (f/stop, 2.5; no optical filter, 4×4 binning). After background correction, the region of interest (area of implantation) was selected and the mean fluorescence intensities for all pixels were calculated using Carestream Molecular Imaging Software, Network Edition 4.5 (Carestream Health) as established earlier [42–43]. Migration of fibrocytes was studied by *in vivo* imaging over 48 hours. Long term affects of the inhibitory agent SB431542 and the resulting fibrocyte interactions were studied out to 14 days.

2.6 Histological analysis

Scaffolds and surrounding tissue were embedded into OCT compound (Sakura, Torrance, CA) and then sectioned using a Leica Cryostat (CM1850, Leica Microsystems). Quantifications of the cellular response at the material interface were performed through H&E staining as previously reported using Image J [14]. Briefly, data are presented as an average of multiple counts taken from H&E stains, with images captured on the skin side of the biomaterial interface. Fibrosis was assessed using both H&E and Masson Trichrome staining. Furthermore, Oil Red O staining was performed to evaluate the accumulation of lipids in the tissue. Briefly, after rinsing in 60% isopropanol, the sections are stained with the working solution of Oil Red O for 15 to 20 minutes. The samples are then counterstained with hematoxylin and used for histological analyses.

The density of fibrocytes ($CD45^+$, collagen I^+), myofibroblasts (α-SMA^+), and adipocytes ($FABP4^+$) around the implant was further assessed using immunohistochemistry. All antibodies were purchased from Santa Cruz Biotech. The appropriate fluorescent secondary antibodies isotype conjugated to either FITC or Texas Red was used for each primary antibody. For all stains, nuclei were visualized using DAPI (Invitrogen, Carlsbad, CA). Interface density of expressing cell was quantified per interface area as previously described [14]. Cell densities were calculated as the number of positive cells per area, approximately similar areas were used in each case calculated from Image J. Stained sections were visualized using a Leica microscope and imaged with a CCD camera (Retiga EXi, Qimaging, Surrey BC, Canada).

2.7 Statistics

GraphPad (La Jolla, CA) was used for all statistical operations. Results are reported as the means ± standard deviations. For all animal studies 6 mice were used for each treatment group. Differences between treatment groups were assessed using ANOVA with Bonferroni comparisons for data with multiple group comparisons. The student's t-test was performed for data with single group comparisons. All data were considered significant when $P<0.05$(*) or $P < 0.01$(**).

3 Results

3.1 Fibrocyte migration is responsive to the biomaterial mediated reaction

We first determined the differentiation of fibrocytes from splenic cells based on morphology and dual expression of the surface markers CD45 and Collagen 1. We find that the fibrocytes stain positive for both CD45 (red) and Collagen 1 (green) and maintain a spindle shaped morphology with a typical oval shaped nucleus. The fibrocyte yield after 7 days in culture was found to be 72 ± 7.1% while approximately 27 ± 8.8% of the cells were found to stain positive for α-SMA (Figure 1a). This is not unexpected, as fibrocytes show an increased expression of α-SMA as they differentiate to fibroblasts or myofibroblasts [15, 44–45]. To keep α-SMA expression at a minimum all cells were used for subsequent testing after only 7 days in culture.

Migration of fibrocytes was confirmed *in vivo* by labeling cells with the NIR fluorophore Xsight 761. Labeled fibrocytes were injected iv and real time monitoring was performed on mice which had previously received a microbubble scaffold implant as a model biomaterial implant. We observed that injected fibrocytes do indeed migrate to the site of implantation over 24 to 48 hours. The response was also observed to increase with time over the PBS controls (Figure 1b). Although made from biocompatible PLGA polymer the scaffold implant is known to elicit an inflammatory response resulting in the formation of a fibrotic capsule as previously demonstrated [23]. This initial study confirms that fibrocytes migrate to an inflammatory site surrounding a subcutaneous biomaterial implant and may be responsive to the biomaterial mediate reaction. To determine if the migratory response and later activation of fibrocytes can be altered to reduce the fibrotic outcome we further assessed the localized inhibition of well known inflammatory and fibrotic mediators IL1-β, TNF-α and TGF-β.

3.2 Localized release of TGF-β inhibitor SB431542 reduces fibrocyte migration

The microbubble scaffold fabrication was altered slightly to incorporate bovine gelatin microbubbles as opposed to previous fabrication with albumin microbubbles. Gelatin is a denatured form of collagen and as such contains a similar chemical structure to glycosaminoglycan and collagen, promoting cell adhesion by mimicking the natural extracellular matrix (ECM) [46]. In opposition, incorporation of albumin, which is an abundant plasma protein, works to passivate the biomaterial surface [47]. Despite this change in scaffold fabrication, characterization of the microbubble scaffolds was in line with previously reported results for the albumin microbubble scaffolds [23]. Briefly, cross sections were analyzed to confirm a macro-porous structure with pores ranging from 50–150 μm, interconnected with smaller pores from lyophilization. Porosity of the microbubble scaffolds was also similarly tested and found to be >90% porous. A representative image of the scaffold is shown in supplemental figure 1a. Due to the solubility of SB431542 and SB203580 in DMSO the drugs were incorporated into the polymer portion of the scaffold as opposed to the protein. This provided prolonged release extending beyond 14 days as demonstrated by HPLC quantification of the release kinetics (Supplemental Figure 1b–d). By incubating the drug-loaded scaffolds with PBS for various periods of time, we determined that the average release rate of SB431542 was approximately 1 μM per day, and that of SB203580 was approximately 10 μM per day. These approximate concentrations have been shown to be effective in reducing the respective cytokines in vitro [24, 27].

The release of TGF-β at the tissue injury site is well known to contribute to the regulation of the fibrotic response [17, 48]. In addition TGF-β has been linked to the increase in the fibrocyte population in several disease states such as aberrant wound healing [49]. To determine an influence on fibrocyte reactions we incorporated the ALK-5 inhibitor SB431542 into scaffolds and studied the fibrocyte migration during localized inhibition of TGF-β. SB431542 has been extensively tested elsewhere and found to have good cytokine specificity for TGF- β [26, 50]. Four hours after implantation with the drug releasing microbubble scaffolds NIR labeled fibrocytes were administered through iv. injection. Real time *in vivo* monitoring was performed to study the migration over 48 hours. As expected, fibrocytes readily migrate to the control scaffold (gelatin microbubble scaffold without drug)

within 24 hours. Interestingly, inhibition of the TGF-β signal significantly reduced the accumulation of fibrocytes around the implant at 24 hours ($P<0.05$) and maintained a 2.5 fold reduction from the control out to 48 hours post injection (Supplemental Figure 1e). Parallel experiments were carried out with the p38 MAPK inhibitor SB203580.While there is some reduction in fibrocyte signal with release of SB203580, the inhibition of IL-1β/TNF-α does not show a statistically relevant difference from the control over 48hrs.

3.3 Effect of cytokine antagonist SB431542 on tissue reactions

We further investigated the effects of the cytokine antagonists on the degree of implantmediated fibrotic tissue reactions. In the long-term response we observe a reduction in the formation of the foreign body capsule with the release of SB431542 (TGF-β antagonist). The microbubble scaffold control is observed to have a capsule thickness of 213 ± 23 μm where localized treatment with SB431542 significantly reduces the capsule thickness to 119 ± 14 μm ($P<0.01$) (Figure 2). Surprisingly, inhibition of IL1-β/TNF-α by SB203580 does not show a significant reduction in capsule thickness (180 ± 24 μm). Using the capsule thickness as a general indicator of the degree of fibrosis we continued to analyze the resultant degree of fibrocytes within the capsule at 14 days post implantation. Similar to the fibrotic capsule results, we observed a marked decrease in the number of fibrocytes surrounding the implants releasing SB431542 but not SB203580 (Figure 2). In addition, we investigated the degree of α-SMA expression and the relative collagen production around the implant as these are considered the hallmarks of activated fibrocytes. It is thought that migratory fibrocytes transition into myofibroblasts losing their hematopoietic expression of CD34 and CD45 and up-regulating α-SMA [18, 51]. Furthermore it has been suggested that this process is mediated by TGF-β expression [31, 52–53]. We found that the inhibition of TGF-β similarly reduced the α-SMA expression significantly ($P<0.01$), and had a resultant influence on the degree of collagen production in the foreign body capsule (Figure 2).

3.4 In vitro fibrocyte to adipocyte differentiation

To investigate the potential of fibrocyte differentiation as an alternative strategy to mitigate fibrosis, we first confirm that stimulation of fibrocytes with an adipogenic medium is capable of prompting differentiation. After the initial culture of fibrocytes from the spleen, cells were incubated with an adipogenic medium for two weeks to stimulate fibrocyte-derived adipocytes. Morphologically, the fibrocyte-derived adipocytes are larger and rounder than the spindle shaped fibrocytes in culture (Figure 3a). To confirm that an adipocyte lineage was obtained, some cells were stained with Oil Red O to observe the accumulation of intracellular lipids. In fact, within the cell population approximately 65–70% of the cells show positive staining for intracellular lipids. In contrast, cells cultured with control media show only nonspecific uptake of the Oil Red O dye. By extracting the dye from both fibrocyte-derived adipocyte samples and control fibrocyte samples we are able to quantify a relative 6 fold increase in the amount of lipid accumulation in the fibrocyte-derived adipocyte cell cultures ($P<0.01$) (Figure 3b). In addition, we also investigated the amount of collagen produced by the fibrocytes and fibrocyte-derived adipocytes using a sirius red staining protocol [41]. The sirius red dye can similarly be extracted to quantify the relative amount of collagen staining in both sets of samples.As expected, the increase in lipid accumulation is mirrored by a 3 fold decrease in the amount

of collagen production in fibrocyte-derived adipocyte cultures ($P<0.01$) (Figure 3c). These findings are in agreement with previous reports indicating that the adipocyte and myofibroblasts differentiation pathways of fibrocytes show reciprocal inhibition of each other [12, 36].

3.5 Fibrocyte to adipocyte stimulation reduces fibrotic outcome in vivo

After confirming that cultured fibrocytes can be stimulated to fibrocyte-derived adipocytes *in vitro*, we continued our investigation of the differentiation capability *in vivo*. To deliver constant and sustained differentiation stimulus, mini-osmotic pumps were connected to the microbubble scaffold implants via catheter tubes. The tissue response to adipogenic stimulation was then assessed at two weeks. By comparing untreated scaffold implant controls to adipogenic treatment and the normal tissue response (subcutaneous area between the hypoderms and the skeletal muscle without the presence of an implant), we find that adipogenic stimulation can significantly alter the fibrotic response. Histological staining by Oil Red O reveals a significant increase in the lipid droplet accumulation throughout the developing tissue under adipogenic stimulation, consistent with an increase in adipogenesis. Furthermore, collagen staining by aniline blue (Masson Trichrome staining) shows a significant reduction in the overall collagen formation with small single fibers running through the tissue in contrast to the large bundles typically observed in the untreated control. In both cases, as expected, the normal tissue response shows scarce lipid droplet accumulation and thin collagen bundles separating the hypodermis from the skeletal muscle (Figure 4a). Interestingly, the lipid and collagen accumulation show similar trends *in vivo* as previously observed *in vitro* with fibrocyte-derived adipocytes. The percentage of lipid staining shows a 2.8 fold increase, from the untreated control, around the implant after 2 weeks (Figure 4b). On the other hand, the collagen percentage is again shown to reflect the increased formation of lipids with a 2.3 fold reduction from the untreated control during adipogenic stimulation. Most importantly, the collagen content in the fibrotic capsule is observed to be reduced down to the levels obtained for normal tissue (Figure 4c). Interestingly while these various trends are observed the overall capsule cell density remains similar for both the treated and untreated scaffold implants (Figure 4d).

The histological results indicate that adipocyte stimulation can block the progressive overproduction of collagen typically observed during the fibrotic response. It is however unclear whether this result is directly linked to fibrocyte -adipocyte stimulation. We therefore further investigated the potential to alter the localized fibrocyte differentiation by assessing both the acute (5 day) and long-term (14 day) response of fibrocytes during adipogenic induction. In the acute response we find that fibrocytes continue to migrate to the implant regardless of adipogenic stimulation. In fact there are no observed differences between the fibrocyte numbers in the untreated vs. treated scaffold samples at day 5 (Figure 5a). In the later response, fibrocytes remain prevalent in the control over 14 days however their presence has been reduced by 4.5 fold during adipogenic differentiation, reducing their numbers down to the level found in normal tissue (Figure 5a). In addition to the reduction of the fibrocyte number within the capsule, we also observe a 51% decrease in the α-SMA expression after adipogenic stimulation over 14 days (Figure 5b). Furthermore, while α-SMA expression is reduced, the mature adipocyte marker, fatty acid binding protein 4

(FABP4) shows a 66% increase in the treated samples from the untreated controls (Figure 5c).

4 Discussion

In the foreign body response a detrimental host reaction, such as the over-expression of extracellular matrix and collagen production, often leads to the separation of implant and healthy tissue by the formation of a thick fibrous capsule. Resident tissue fibroblasts have long been the primary suspect for dictating this deleterious effect. Recently, fibroblast-like cells termed fibrocytes, have shown an increasing importance in connection with fibrosis in several fibrotic disease models [54–56]. We show here that fibrocytes indeed play a role in the biomaterial-mediated reaction as well. To begin with, cultured fibrocytes are shown to migrate to the site of biomaterial implantation and respond to the biomaterial-mediated reaction. To culture fibrocytes *in vitro* peripheral blood mononuclear cells may be isolated and differentiated into fibrocytes [53]. There are however a low number of circulating monocytes found in blood and the blood from multiple mice must be pooled together to obtain an adequate number of cells [37, 53]. More recently, fibrocytes have been shown to differentiate from the splenic reservoir of monocytes [37, 57]. With proper conditioning, a larger number of cells may be isolated and differentiated to fibrocytes from a single mouse spleen. This source has the potential to generate substantial numbers of fibrocytes from a small number of animals.

To further understand and alter the migratory and activation state of fibrocytes we first focused on the fibrotic regulatory cytokine TGF-β which is up-regulated during an inflammatory or wound healing response. It is well documented that pro-inflammatory cytokines such as IL-1β, IL-6, IL-12 and TNF-α are initially expressed in high quantities in response to a biomaterial implant [2, 11]. As inflammation shifts to regeneration however there is a shift in cytokine and growth factor release to more anti-inflammatory and pro-fibrotic cytokines such as IL-10 and TGF-β [2, 11]. The migratory response of fibrocytes may be dependent on this shift in signaling cues, such as increased TGF-β production. Indeed, studies have shown that TGF-β is a potent initiator of fibrotic reactions, as well as a stimulant for fibroblasts and macrophages to up-regulate pro-fibrotic growth factor expression [16]. Along these lines, many recent studies have indicated that fibrocytes are responsive to TGF-β increasing accumulation and differentiation [31, 52–53]. We therefore sought to deter TGF-β mediated fibrocyte responses through localized release of the TGF-β antagonist SB431542. In the acute response, the migration of NIR labeled fibrocytes is significantly reduced over 48 hours with the release of SB431542. During the long-term response, in addition to a reduction of capsule thickness, we observe a significant decrease in the fibrocyte numbers as well as the α-SMA expression surrounding the implants. Increased α -SMA expression is a known hallmark for myofibroblast differentiation and fibrocytes have been well characterized to differentiate to myofibroblasts under TGF-β stimulation *in vitro* [18]. Our results therefore indicate that the differentiation of fibrocytes into α-SMA expressing myofibroblasts can be significantly reduced by the TGF-β antagonist SB431542. While the results are promising and demonstrate a reduction in fibrocyte responses, the overall collagen production was not significantly reduced from the control. This observation may indicate that alternative pathways beyond the TGF-β influence are

also involved. Interestingly, IL-1β and TNF-α antagonist SB203580 had less of an effect on the degree and response of fibrocyte infiltration. IL-1 and TNF-α are known to be potent inflammatory mediators, however there is also some evidence that they can play a role in stimulating fibrosis and collagen production. In two separate studies of bleomycin induced pulmonary fibrosis both IL-1 and TNF-α were found to be stimulatory for the growth of fibroblasts and localized collagen deposition [58–59]. Our results indicate however that the inflammatory signal from IL-1 and TNF-α may not have a major influence on fibrocytes. Overall, the percentage of collagen production surrounding the implant was not significantly impacted by the pharmacokinetic approach. This is likely due to several contributing alternative mechanisms which influence fibrocyte and resident tissue fibroblast responses. Indeed, several mechanisms have been identified for fibrocyte migration [15, 19, 60], activation [32, 53, 61], and even differentiation [12–13, 62]. The complex cascade and complimentary interactions between various cell responses support that a new and different approach is needed to alter fibrotic tissue reactions to biomaterial implants. We therefore sought an alternative approach to pharmacokinetic inhibition that could potentially overcome the combination of different mechanisms. We hypothesized that a more direct strategy specifically targeting the differentiation aspect of fibrocytes would have a greater impact on the fibrotic response and localized collagen production.

To confirm our hypothesis we investigated the capability of fibrocytes to dif ferentiate to an adipocyte lineage under specific culture conditions. Our results show that the cells were observed to increase in size and adapt a round morphology, in opposition to spindle shaped fibrocytes, as well as increase intracellular lipid production after adipocyte stimulation. Additionally, we observed a corresponding decrease in collagen production from fibrocyte-derived adipocytes *in vitro*. In support of this observation, a previous study has indicated that the fibrocyte-to-adipocyte differentiation is driven by PPARγ which was shown to reduce α-SMA expression [12]. Furthermore, *in vitro* stimulation with TGF-β was shown to inhibit fibrocyte-to-adipocyte differentiation [12]. These interactions demonstrate an intriguing ability of fibrocytes, where increased adipocyte stimulation could reciprocally reduce collagen formation, ultimately impacting the fibrotic responses and scar tissue formation. In support of this notion, a previous study was able to show the formation of human adipose tissue in SCID mice after 4 weeks with the implantation human fibrocyte-derived adipocytes [13]. In this study however fibrocytes were stimulated *in vitro* to adipocytes prior to *in vivo* implantation. Nevertheless, the study does indicate that fibrocyte-derived adipocytes can develop adipose tissue *in vivo* [13].

Our *in vivo* investigations suggest that fibrocytes may indeed be stimulated to differentiate into adipocytes around subcutaneous biomaterial implants. Fibrocytes were first indentified to migrate to the adipogenic samples during the acute inflammatory response. Subsequently, while the fibrocyte numbers continually increase around the untreated samples, the adipogenic samples show a significant decrease in fibrocyte numbers over two weeks. An observed decrease would be expected with adipocyte differentiation as fibrocytes are known to decrease expression of hematopoietic markers CD45 and CD34 during differentiation [15, 44– 45]. Furthermore, a similar reduction is observed in the overall α-SMA expression indicating the loss of fibrocytes is not due to myofibroblast differentiation. The observed

reduction in α-SMA expression is further confirmed by the significant decrease in collagen production around the adipogenic samples. In fact, the total collagen content has been reduced down to the level found in normal tissue. This indicates that stimulated fibrocyte-to-adipocyte differentiation may inhibit fibrocyte-to-myofibroblast differentiation and over production of collagen. Finally, fibrocyte-to-adipocyte differentiation is further supported by the significant increase in FABP4 expression in the cells surrounding the treated implants as well as the observed increase in lipid accumulation within the capsule.

While these findings all support the *in vivo* differentiation of fibrocytes to adipocytes, we cannot rule out other potential mediators. For instance, it is possible that the resultant increase in lipid accumulation is a result of stem cell recruitment and subsequent differentiation to adipocytes rather than fibrocyte-derived adipocytes. More in-depth studies such as chimeric models or labeled fibrocytes would need to be conducted to conclusively demonstrate fibrocyte-derived adipocytes *in vivo*. We believe however that our results present the first evidence that the differentiation potential of fibrocytes is a viable strategy to alter fibrotic tissue responses to biomaterial implants. In addition, we believe this approach may offer potential benefits to address and overcome certain issues and complications. For example, in wound healing the use of inhibitors for factors like TFG-β may have a significant adverse effect altering the wound regeneration including the recruitment and differentiation of cells. Furthermore, surrounding an implant with adipose tissue could have potential benefits for some devices. For an implant such as a drug releasing capsule, it is feasible that the highly vascularized native structure of adipose tissue would help facilitate compound release and uptake into the blood stream and surrounding tissue. Nevertheless, further investigation of such processes and applications could lead to enhanced strategies for site specific modulation and regeneration of site specific tissue.

5 Conclusion

Understanding and manipulating fibrocyte interactions is becoming increasingly important as a means to mitigate fibrosis. Our results suggest that fibrocytes play a critical role in biomaterial mediated fibrotic responses and are augmented by TGF-β. In both the acute and long-term tissue response to subcutaneous scaffold implants the localized inhibition of TGF-β by SB431542 was able to reduce the fibrocyte migration and deter myofibroblast differentiation. In an alternative strategy we demonstrate that the multi-potent capacity of fibrocytes may be specifically targeted to reduce collagen formation. Fibrocyte-derived adipocytes show enhanced intracellular lipid production *in vitro* with a reflected reduction in collagen accumulation. Similarly, *in vivo* adipogenic stimulation resulted in enhanced lipid formation and significant collagen reduction around treated scaffolds. Furthermore, the adipogenic samples show minimal fibrocyte and myofibroblast accumulation leading us to infer that adipocyte stimulation passivates the fibrotic potential of immigrated fibrocytes. To the best of our knowledge, this study presents the first evidence that the differentiation potential of fibrocytes is a viable strategy to alter fibrotic tissue responses to biomaterial implants. Further study is needed however to investigate fibrocyte interactions and conclusively demonstrate that fibrocyte-derived adipocytes can lead to a reduction in the collagen content and scar tissue formation to improve the safety and function of medical implants.

Supplementary Material

Refer to Web version on PubMed Central for supplementary material.

Acknowledgments

This work was supported by NIH grant RO1 EB007271 and EB014404.

References

1. Tuan RS, Lee FY, T Konttinen Y, Wilkinson JM, Smith RL. What are the local and systemic biologic reactions and mediators to wear debris, and what host factors determine or modulate the biologic response to wear particles? J Am Acad Orthop Surg. 2008; 16(Suppl 1):S42–S48. [PubMed: 18612013]
2. Anderson JM, Rodriguez A, Chang DT. Foreign body reaction to biomaterials. Semin Immunol. 2008; 20:86–100. [PubMed: 18162407]
3. Jones JA, Chang DT, Meyerson H, Colton E, Kwon IK, Matsuda T, et al. Proteomic analysis and quantification of cytokines and chemokines from biomaterial surface-adherent macrophages and foreign body giant cells. J Biomed Mater Res A. 2007; 83:585–596. [PubMed: 17503526]
4. Kou PM, Babensee JE. Macrophage and dendritic cell phenotypic diversity in the context of biomaterials. J Biomed Mater Res A. 2010
5. Thomsen P, Gretzer C. Macrophage interactions with modified material surfaces. Curr Opin Solid St M. 2001; 5:163–176.
6. Darby IA, Hewitson TD. Fibroblast differentiation in wound healing and fibrosis. Int Rev Cytol. 2007; 257:143–179. [PubMed: 17280897]
7. Luttikhuizen DT, Dankers PY, Harmsen MC, van Luyn MJ. Material dependent differences in inflammatory gene expression by giant cells during the foreign body reaction. J Biomed Mater Res A. 2007; 83:879–886. [PubMed: 17567860]
8. Chan A, Filer A, Parsonage G, Kollnberger S, Gundle R, Buckley CD, et al. Mediation of the proinflammatory cytokine response in rheumatoid arthritis and spondylarthritis by interactions between fibroblast-like synoviocytes and natural killer cells. Arthritis Rheum. 2008; 58:707–717. [PubMed: 18311795]
9. Chang DT, Jones JA, Meyerson H, Colton E, Kwon IK, Matsuda T, et al. Lymphocyte/macrophage interactions: biomaterial surface-dependent cytokine, chemokine, and matrix protein production. J Biomed Mater Res A. 2008; 87:676–687. [PubMed: 18200554]
10. Reilkoff RA, Bucala R, Herzog EL. Fibrocytes: emerging effector cells in chronic inflammation. Nat Rev Immunol. 2011; 11:427–435. [PubMed: 21597472]
11. Ward WK. A Review of the Foreign-body Response to Subcutaneously-implanted Devices: The Role of Macrophages and Cytokines in Biofouling and Fibrosis. Journal of Diabetes Science and Technology. 2008; 2:768–777. [PubMed: 19885259]
12. Hong KM, Belperio JA, Keane MP, Burdick MD, Strieter RM. Differentiation of human circulating fibrocytes as mediated by transforming growth factor-beta and peroxisome proliferator-activated receptor gamma. J Biol Chem. 2007; 282:22910–22920. [PubMed: 17556364]
13. Hong KM, Burdick MD, Phillips RJ, Heber D, Strieter RM. Characterization of human fibrocytes as circulating adipocyte progenitors and the formation of human adipose tissue in SCID mice. FASEB J. 2005; 19:2029–2031. [PubMed: 16188961]
14. Thevenot PT, Baker DW, Weng H, Sun MW, Tang L. The pivotal role of fibrocytes and mast cells in mediating fibrotic reactions to biomaterials. Biomaterials. 2011; 32:8394–8403. [PubMed: 21864899]
15. Phillips RJ, Burdick MD, Hong K, Lutz MA, Murray LA, Xue YY, et al. Circulating fibrocytes traffic to the lungs in response to CXCL12 and mediate fibrosis. J Clin Invest. 2004; 114:438–446. [PubMed: 15286810]

16. Mulsow JJ, Watson RW, Fitzpatrick JM, O'Connell PR. Transforming growth factor-beta promotes pro-fibrotic behavior by serosal fibroblasts via PKC and ERK1/2 mitogen activated protein kinase cell signaling. Ann Surg. 2005; 242:880–887. discussion 7–9. [PubMed: 16327498]
17. Bakhshayesh M, Soleimani M, Mehdizadeh M, Katebi M. Effects of TGF-beta and b-FGF on the potential of peripheral blood-borne stem cells and bone marrow-derived stem cells in wound healing in a murine model. Inflammation. 2012; 35:138–142. [PubMed: 21274741]
18. Schmidt M, Sun G, Stacey MA, Mori L, Mattoli S. Identification of circulating fibrocytes as precursors of bronchial myofibroblasts in asthma. J Immunol. 2003; 171:380–389. [PubMed: 12817021]
19. Moore BB, Murray L, Das A, Wilke CA, Herrygers AB, Toews GB. The role of CCL12 in the recruitment of fibrocytes and lung fibrosis. Am J Respir Cell Mol Biol. 2006; 35:175–181. [PubMed: 16543609]
20. Mehrad B, Burdick MD, Strieter RM. Fibrocyte CXCR4 regulation as a therapeutic target in pulmonary fibrosis. Int J Biochem Cell Biol. 2009; 41:1708–1718. [PubMed: 19433312]
21. Phan SH. Biology of fibroblasts and myofibroblasts. Proc Am Thorac Soc. 2008; 5:334–337. [PubMed: 18403329]
22. Tomasek JJ, Gabbiani G, Hinz B, Chaponnier C, Brown RA. Myofibroblasts and mechano-regulation of connective tissue remodelling. Nat Rev Mol Cell Biol. 2002; 3:349–363. [PubMed: 11988769]
23. Nair A, Thevenot P, Dey J, Shen J, Sun MW, Yang J, et al. Novel polymeric scaffolds using protein microbubbles as porogen and growth factor carriers. Tissue Eng Part C Methods. 2010; 16:23–32. [PubMed: 19327002]
24. Waghabi MC, de Souza EM, de Oliveira GM, Keramidas M, Feige JJ, Araujo-Jorge TC, et al. Pharmacological inhibition of transforming growth factor beta signaling decreases infection and prevents heart damage in acute Chagas' disease. Antimicrob Agents Chemother. 2009; 53:4694–4701. [PubMed: 19738024]
25. Xiao YQ, Liu K, Shen JF, Xu GT, Ye W. SB-431542 inhibition of scar formation after filtration surgery and its potential mechanism. Invest Ophthalmol Vis Sci. 2009; 50:1698–1706. [PubMed: 19098325]
26. Laping NJ, Grygielko E, Mathur A, Butter S, Bomberger J, Tweed C, et al. Inhibition of transforming growth factor (TGF)-beta1-induced extracellular matrix with a novel inhibitor of the TGF-beta type I receptor kinase activity: SB-431542. Mol Pharmacol. 2002; 62:58–64. [PubMed: 12065755]
27. Badger AM, Bradbeer JN, Votta B, Lee JC, Adams JL, Griswold DE. Pharmacological profile of SB 203580, a selective inhibitor of cytokine suppressive binding protein/p38 kinase, in animal models of arthritis, bone resorption, endotoxin shock and immune function. J Pharmacol Exp Ther. 1996; 279:1453–1461. [PubMed: 8968371]
28. Kagari T, Doi H, Shimozato T. The importance of IL-1 beta and TNF-alpha, and the noninvolvement of IL-6, in the development of monoclonal antibody-induced arthritis. J Immunol. 2002; 169:1459–1466. [PubMed: 12133972]
29. Zhou WD, Yang HM, Wang Q, Su DY, Liu FA, Zhao M, et al. SB203580, a p38 mitogen-activated protein kinase inhibitor, suppresses the development of endometriosis by down-regulating proinflammatory cytokines and proteolytic factors in a mouse model. Hum Reprod. 2010; 25:3110–3116. [PubMed: 20956267]
30. Jin N, Wang Q, Zhang X, Jiang D, Cheng H, Zhu K. The selective p38 mitogen-activated protein kinase inhibitor, SB203580, improves renal disease in MRL/lpr mouse model of systemic lupus. Int Immunopharmacol. 2011; 11:1319–1326. [PubMed: 21549858]
31. Bellini A, Mattoli S. The role of the fibrocyte, a bone marrow-derived mesenchymal progenitor, in reactive and reparative fibroses. Lab Invest. 2007; 87:858–870. [PubMed: 17607298]
32. Chesney J, Metz C, Stavitsky AB, Bacher M, Bucala R. Regulated production of type I collagen and inflammatory cytokines by peripheral blood fibrocytes. J Immunol. 1998; 160:419–425. [PubMed: 9551999]

33. Hong KM, Burdick MD, Phillips RJ, Heber D, Strieter RM. Characterization of human fibrocytes as circulating adipocyte progenitors and the formation of human adipose tissue in SCID mice. Faseb Journal. 2005; 19:2029-+. [PubMed: 16188961]
34. Choi YH, Burdick MD, Strieter RM. Human circulating fibrocytes have the capacity to differentiate osteoblasts and chondrocytes. Int J Biochem Cell B. 2010; 42:662–671.
35. Koumas L, Smith TJ, Feldon S, Blumberg N, Phipps RP. Thy-1 expression in human fibroblast subsets defines myofibroblastic or lipofibroblastic phenotypes. American Journal of Pathology. 2003; 163:1291–1300. [PubMed: 14507638]
36. Burgess HA, Daugherty LE, Thatcher TH, Lakatos HF, Ray DM, Redonnet M, et al. PPAR gamma agonists inhibit TGF-beta induced pulmonary myofibroblast differentiation and collagen production: implications for therapy of lung fibrosis. Am J Physiol-Lung C. 2005; 288:L1146–L1153.
37. Crawford JR, Pilling D, Gomer RH. Improved serum-free culture conditions for spleen-derived murine fibrocytes. J Immunol Methods. 2010; 363:9–20. [PubMed: 20888336]
38. Nair A, Shen J, Lotfi P, Ko CY, Zhang CC, Tang L. Biomaterial implants mediate autologous stem cell recruitment in mice. Acta Biomater. 2011; 7:3887–3895. [PubMed: 21784181]
39. Thevenot PT, Nair AM, Shen J, Lotfi P, Ko CY, Tang L. The effect of incorporation of SDF-1alpha into PLGA scaffolds on stem cell recruitment and the inflammatory response. Biomaterials. 2010; 31:3997–4008. [PubMed: 20185171]
40. Ramirez-Zacarias JL, Castro-Munozledo F, Kuri-Harcuch W. Quantitation of adipose conversion and triglycerides by staining intracytoplasmic lipids with Oil red O. Histochemistry. 1992; 97:493–497. [PubMed: 1385366]
41. Tullberg-Reinert H, Jundt G. In situ measurement of collagen synthesis by human bone cells with a sirius red-based colorimetric microassay: effects of transforming growth factor beta2 and ascorbic acid 2-phosphate. Histochem Cell Biol. 1999; 112:271–276. [PubMed: 10550611]
42. Zhou JT, Y Weng H, Tang L. Noninvasive assessment of localized inflammatory responses. Free Radical Biology and Medicine. 2011
43. Zhou J, Tsai YT, Weng H, Baker DW, Tang L. Real time monitoring of biomaterial-mediated inflammatory responses via macrophage-targeting NIR nanoprobes. Biomaterials. 2011; 32:9383–9390. [PubMed: 21893338]
44. Moore BB, Kolodsick JE, Thannickal VJ, Cooke K, Moore TA, Hogaboam C, et al. CCR2-mediated recruitment of fibrocytes to the alveolar space after fibrotic injury. Am J Pathol. 2005; 166:675–684. [PubMed: 15743780]
45. Quan TE, Cowper S, Wu SP, Bockenstedt LK, Bucala R. Circulating fibrocytes: collagen-secreting cells of the peripheral blood. Int J Biochem Cell Biol. 2004; 36:598–606. [PubMed: 15010326]
46. Gu ZX, Kong L, Feng X, Guo T, Dai J, Li S, et al. Synthesis and characterization of PLGA-gelatin complex with growth factor incorporation as potential matrix. J Alloy Compd. 2009; 474:450–454.
47. Tang LP, Eaton JW. Fibrin(Ogen) Mediates Acute Inflammatory Responses to Biomaterials. J Exp Med. 1993; 178:2147–2156. [PubMed: 8245787]
48. Seppa H, Grotendorst G, Seppa S, Schiffmann E, Martin GR. Platelet-Derived Growth-Factor Is Chemotactic for Fibroblasts. Journal of Cell Biology. 1982; 92:584–588. [PubMed: 7061598]
49. Yang L, Scott PG, Giuffre J, Shankowsky HA, Ghahary A, Tredget EE. Peripheral blood fibrocytes from burn patients: identification and quantification of fibrocytes in adherent cells cultured from peripheral blood mononuclear cells. Lab Invest. 2002; 82:1183–1192. [PubMed: 12218079]
50. Lavoie P, Robitaille G, Agharazii M, Ledbetter S, Lebel M, Lariviere R. Neutralization of transforming growth factor-beta attenuates hypertension and prevents renal injury in uremic rats. J Hypertens. 2005; 23:1895–1903. [PubMed: 16148614]
51. Mori L, Bellini A, Stacey MA, Schmidt M, Mattoli S. Fibrocytes contribute to the myofibroblast population in wounded skin and originate from the bone marrow. Exp Cell Res. 2005; 304:81–90. [PubMed: 15707576]
52. Metz CN. Fibrocytes: a unique cell population implicated in wound healing. Cell Mol Life Sci. 2003; 60:1342–1350. [PubMed: 12943223]

53. Abe R, Donnelly SC, Peng T, Bucala R, Metz CN. Peripheral blood fibrocytes: differentiation pathway and migration to wound sites. J Immunol. 2001; 166:7556–7562. [PubMed: 11390511]
54. Keeley EC, Mehrad B, Strieter RM. Fibrocytes: bringing new insights into mechanisms of inflammation and fibrosis. Int J Biochem Cell Biol. 2010; 42:535–542. [PubMed: 19850147]
55. Strieter RM, Keeley EC, Hughes MA, Burdick MD, Mehrad B. The role of circulating mesenchymal progenitor cells (fibrocytes) in the pathogenesis of pulmonary fibrosis. J Leukoc Biol. 2009; 86:1111–1118. [PubMed: 19581373]
56. Wada T, Sakai N, Matsushima K, Kaneko S. Fibrocytes: a new insight into kidney fibrosis. Kidney Int. 2007; 72:269–273. [PubMed: 17495856]
57. Niedermeier M, Reich B, Rodriguez Gomez M, Denzel A, Schmidbauer K, Gobel N, et al. CD4+ T cells control the differentiation of Gr1+ monocytes into fibrocytes. Proc Natl Acad Sci U S A. 2009; 106:17892–17897. [PubMed: 19815530]
58. Piguet PF, Collart MA, Grau GE, Kapanci Y, Vassalli P. Tumor Necrosis Factor Cachectin Plays a Key Role in Bleomycin-Induced Pneumonopathy and Fibrosis. J Exp Med. 1989; 170:655–663. [PubMed: 2475571]
59. Piguet PF, Vesin C, Grau GE, Thompson RC. Interleukin-1 Receptor Antagonist (Il-1ra) Prevents or Cures Pulmonary Fibrosis Elicited in Mice by Bleomycin or Silica. Cytokine. 1993; 5:57–61. [PubMed: 7683505]
60. Sakai N, Wada T, Yokoyama H, Lipp M, Ueha S, Matsushima K, et al. Secondary lymphoid tissue chemokine (SLC/CCL21)/CCR7 signaling regulates fibrocytes in renal fibrosis. Proc Natl Acad Sci U S A. 2006; 103:14098–14103. [PubMed: 16966615]
61. Ishida Y, Kimura A, Kondo T, Hayashi T, Ueno M, Takakura N, et al. Essential roles of the CC chemokine ligand 3-CC chemokine receptor 5 axis in bleomycin-induced pulmonary fibrosis through regulation of macrophage and fibrocyte infiltration. Am J Pathol. 2007; 170:843–854. [PubMed: 17322370]
62. Choi YH, Burdick MD, Strieter RM. Human circulating fibrocytes have the capacity to differentiate osteoblasts and chondrocytes. Int J Biochem Cell Biol. 2010; 42:662–671. [PubMed: 20034590]

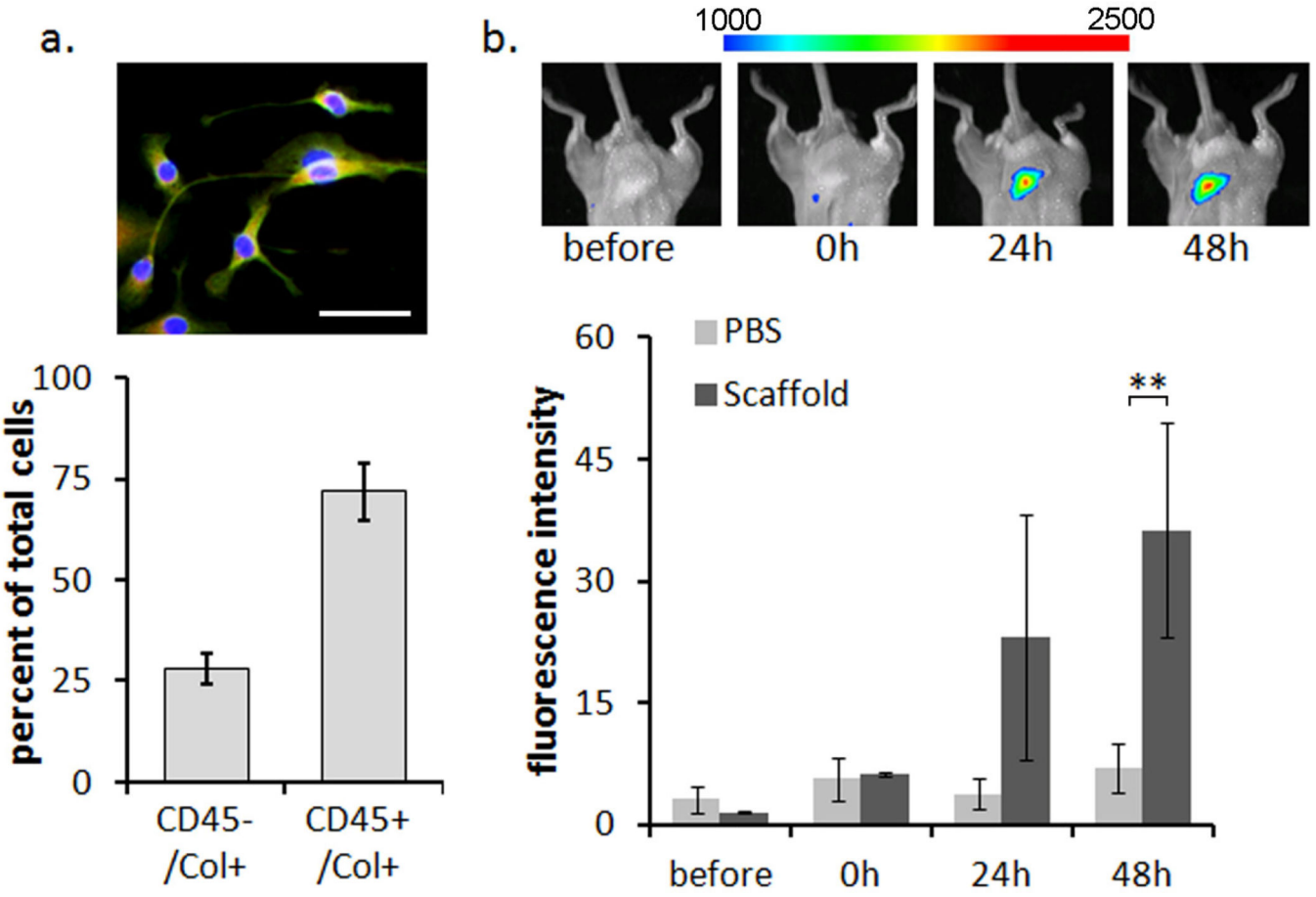

Figure 1.

Confirmation of fibrocyte lineage and migration to the implant site. (A) cultured fibrocytes are positively identified as $CD45^+$ /Col 1^+ by immunohistochemistry. Image shows $CD45^+$ $Col1^+$ cells (yellow) with two cells that are $CD45^-$ $Col1^+$(green). The scale bar represents 50 μm. The bar graph shows that on average, 72% of cultured splenic cells stain positive for fibrocyte markers. (B) NIR labeled fibrocytes, injected iv, migrate to the site of biomaterial scaffold implantation over time. Images show representative fluorescence at the scaffold implant site. The spectrum bar shows the relative fluorescence intensity. Statistics are performed with the student's t-test and taken as significant in at **P<0.01.

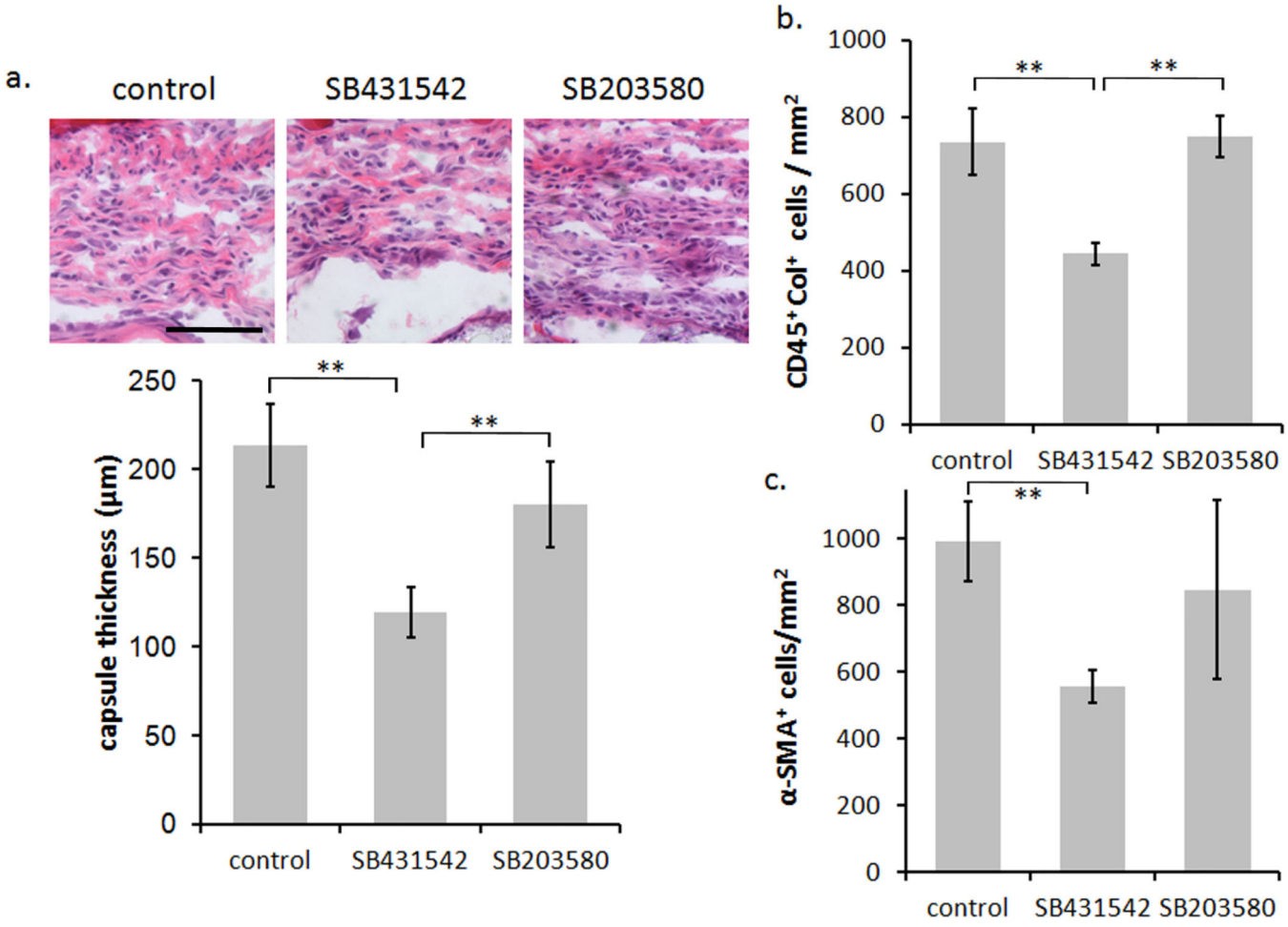

Figure 2.

Long-term response of SB431542 and SB203580 release from scaffold implants. (A) Histological results of H&E staining showing the capsule thickness of the various treatments at 14 days. The scale bar shows 100 μm and is applicable to all images in the panel. (B) Bar graph of the CD45-Col fibrocyte response. (C) Bar graph of the degree of α-SMA positive cells present in the foreign body capsule. In each bar graph the tissue and cellular response to SB431542 was found to be significant from the control. For each treatment group six animals were tested. Statistics are performed by ANOVA with Bonferroni comparisons and taken to be significant at **P<0.01.

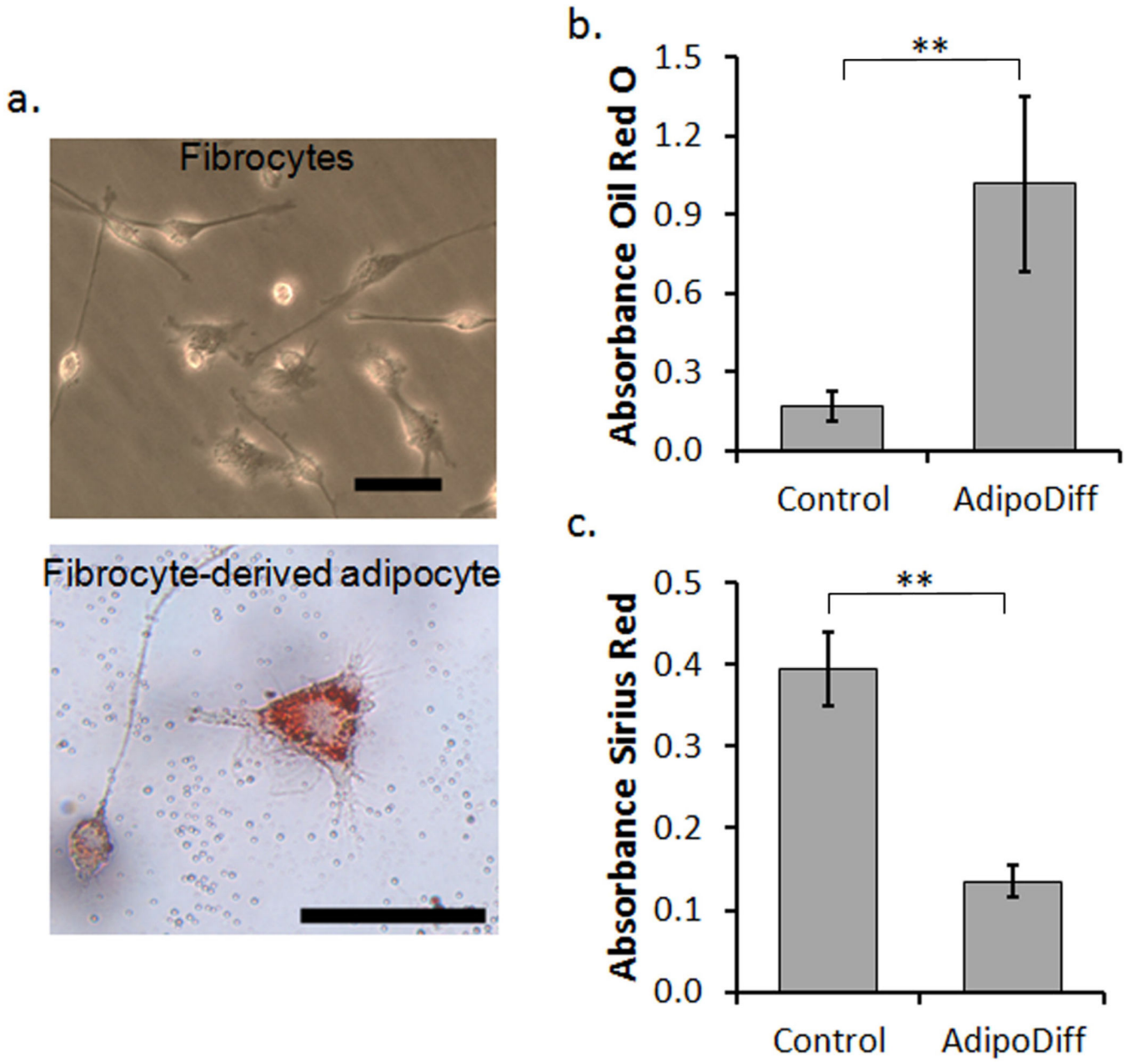

Figure 3.

In vitro differentiation of fibrocytes to an adipocyte-like lineage. (a) Representative images of fibrocytes in culture (top) showing typical spindle morphology and fibrocyte-derived adipocytes (bottom) with increased cell size and spreading as well as the accumulation of lipid droplets stained by Oil Red O. The scale bars represent 50 μm. (b) Quantitative measurements of lipid staining by Oil Red O measured by absorbance of extracted dye. (c) Quantitative measurements of collagen staining by Sirius Red measured by absorbance of extracted dye. Statistics are performed with the student's t-test and taken to be significant at **P<0.01.

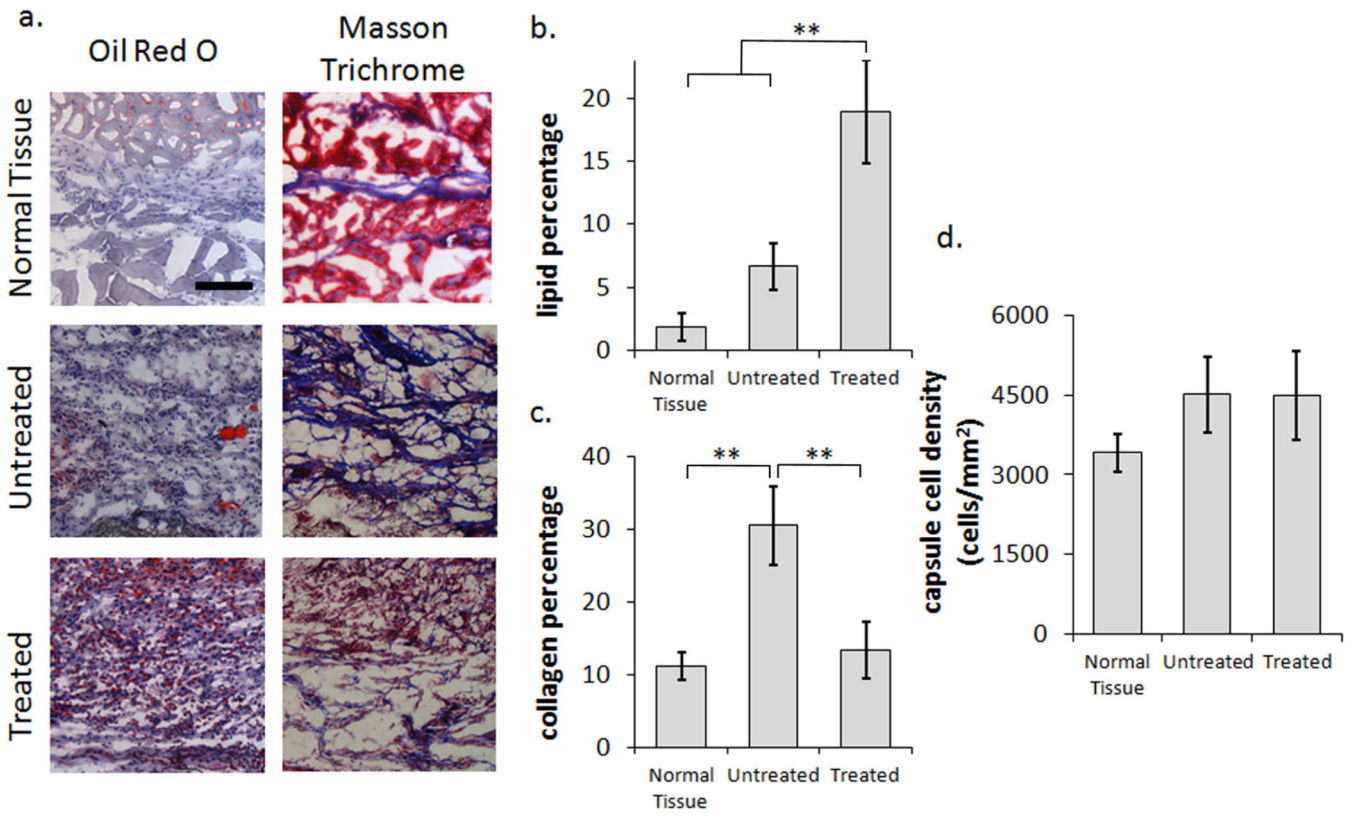

Figure 4.

Histological analysis of fibrocyte-adipocyte differentiation. (a) Panel presenting representative images of Oil Red O and Masson Trichrome staining for Normal Tissue, Untreated, and Treated samples at 2 weeks. The scale bar represents 100 μm and is applicable to all images in the panel. (b) Analysis of lipid accumulation by oil red o staining shows a 2.8 fold increase after Adipogenic stimulation in comparison to the untreated control. (c) The collagen percentage similarly shows a 2.3 fold decrease from the untreated control, however is more importantly observed to be reduced down to the levels obtained for normal tissue. (d) The overall cellular response of the untreated and treated scaffolds remains similar, indicating a shift in the cellular composition between the two, rather than a reduction of the inflammatory response. Six animals were used in each treatment group. Statistics are performed with ANOVA using Bonferroni comparisons and taken to be significant at **$P<0.01$.

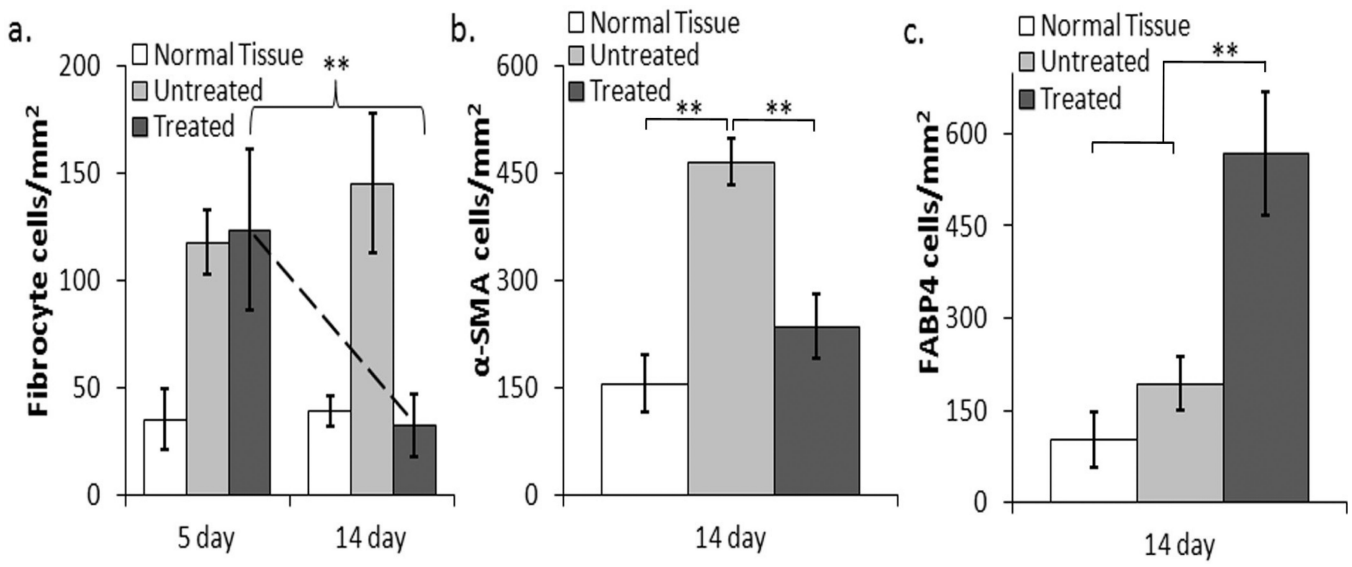

Figure 5.

Quantification of fibrocytes, myofibroblasts expression (α-SMA), and adipocyte expression (FABP4) during adipogenic differentiation. (a) The acute fibrocyte response shows approximately equal recruitment to both the untreated and treated scaffold samples, where the 14 day response shows a drastic reduction in the fibrocyte numbers surrounding the treated scaffold implants. (b) After 14 days, the α-SMA expression levels are significantly reduced during treatment from the untreated scaffold samples and remain within the range of the normal tissue response. (c) As anticipated, after 14 days the adipogenic marker FABP4 expression levels are significantly increased on the treated samples. Six animals were used in each treatment group. Statistics are performed with ANOVA using Bonferroni comparisons and taken to be significant at **$P<0.01$.